Contents lists available at ScienceDirect

Physics Letters B

www.elsevier.com/locate/physletb

PHYSICS LETTERS B

The infrared limit of the SRG evolution and Levinson's theorem

E. Ruiz Arriola [a],*, S. Szpigel [b], V.S. Timóteo [c]

[a] *Departamento de Física Atómica, Molecular y Nuclear and Instituto Carlos I de Física Teórica y Computacional, Universidad de Granada, E-18071 Granada, Spain*
[b] *Centro de Rádio-Astronomia e Astrofísica Mackenzie, Escola de Engenharia, Universidade Presbiteriana Mackenzie, Brazil*
[c] *Grupo de Óptica e Modelagem Numérica – GOMNI, Faculdade de Tecnologia – FT, Universidade Estadual de Campinas – UNICAMP, Brazil*

A R T I C L E   I N F O

A B S T R A C T

On a finite momentum grid with N integration points p_n and weights w_n ($n = 1, \ldots, N$) the Similarity Renormalization Group (SRG) with a given generator G unitarily evolves an initial interaction with a cutoff λ on energy differences, steadily driving the starting Hamiltonian in momentum space $H^0_{n,m} = p_n^2 \delta_{n,m} + V_{n,m}$ to a diagonal form in the infrared limit ($\lambda \to 0$), $H^{G,\lambda \to 0}_{n,m} = E_{\pi(n)} \delta_{n,m}$, where $\pi(n)$ is a permutation of the eigenvalues E_n which depends on G. Levinson's theorem establishes a relation between phase-shifts $\delta(p_n)$ and the number of bound-states, n_B, and reads $\delta(p_1) - \delta(p_N) = n_B \pi$. We show that unitarily equivalent Hamiltonians on the grid generate reaction matrices which are compatible with Levinson's theorem but are phase-inequivalent along the SRG trajectory. An isospectral definition of the phase-shift in terms of an energy-shift is possible but requires in addition a proper ordering of states on a momentum grid such as to fulfill Levinson's theorem. We show how the SRG with different generators G induces different isospectral flows in the presence of bound-states, leading to distinct orderings in the infrared limit. While the Wilson generator induces an ascending ordering incompatible with Levinson's theorem, the Wegner generator provides a much better ordering, although not the optimal one. We illustrate the discussion with the nucleon–nucleon (NN) interaction in the $^1S_0$ and $^3S_1$ channels.

1. Introduction

During the last decade the renormalization group equations have advantageously been used as a technique to simplify microscopic large scale calculations in Nuclear Structure and Reactions. More specifically, the Similarity Renormalization Group (SRG) has been intensively applied to handle multinucleon forces in order to soften the short-distance core [1,2] with a rather universal pattern for nuclear symmetries [3,4] and interactions [5]. The basic strategy underlying the SRG method is to evolve a starting (bare) interaction H_0 which has been fitted to nucleon–nucleon (NN) scattering data via a continuous unitary transformation that runs a cutoff λ on energy differences. Such a transformation generates a family of unitarily equivalent smooth interactions $H_\lambda = U_\lambda H_0 U_\lambda^\dagger$ with a band-diagonal structure of a prescribed width roughly given by the SRG cutoff λ. For most cases of interest a finite momentum grid with N integration points p_n and resolution weights $\Delta p_n = w_n$ ($n = 1, \ldots, N$) is needed to solve the SRG flow equations numerically, and for such a finite basis the SRG

transformation corresponds to a continuum generalization of the well-known Gauss reduction method of a matrix to the diagonal form. Typical calculations have taken $w_n \sim 0.01$ fm^{-1}, $\lambda \sim 2$ fm^{-1} and $N \sim 200$ [1,2]. For reasons to be elaborated below we will analyze here a quite different regime, namely smaller SRG cut-offs and grids, so our discussion will have no implications for the many existing calculations.

Unfortunately the NN force is not yet known from first principles and most information on the NN interaction is strongly constrained by the abundant np and pp scattering data (see e.g. Ref. [6] for a recent upgrade and references therein). Roughly speaking this is equivalent to knowing the phase-shifts with their uncertainties at some center-of-mass (CM) momenta and in a given range, $0 < \Delta p \equiv p_1 < \cdots < p_N \equiv \Lambda$, and in fact a common practice has been to tabulate the phase-shifts at given discrete set of energy values. The implicit assumption underlying this practice is that one expects this discrete information to encode and summarize sufficient details on the interaction, in full harmony with the need of solving SRG flow equations on a finite grid. The computational advantages of using properly chosen few discrete variables for finite volume systems such as nuclei [7] have been emphasized as the number of states gets drastically reduced.

* Corresponding author.
E-mail addresses: earriola@ugr.es (E.R. Arriola), szpigel@mackenzie.br (S. Szpigel), varese@ft.unicamp.br (V.S. Timóteo).

In a previous note [8] we have suggested to pursue this SRG transformation to the very limit since this naturally drives the interaction to a diagonal form and hence removing all off-shell ambiguities. As a consequence the induced three-body forces dominate (for a recent treatment in momentum space see [9]). The two most common choices for the SRG generator which guarantee that the SRG flow equations evolve the Hamiltonian to the diagonal form are the so-called Wegner and Wilson generators. The non-trivial question pertains the ordering of states arising in general from any diagonalization procedure and from the SRG flow equations in particular. On a finite momentum grid the SRG evolution with both Wilson and Wegner generators can drive the Hamiltonian to the diagonal form when $\lambda \to 0$ (unless degeneracies appear in the diagonal). However, in the case of Wegner generator all $N!$ possible permutations corresponding to the final ordering of the eigenvalues are stable fixed points while in the case of Wilson generator only the permutation in which the eigenvalues are in ascending order is a stable fixed point. A perturbative asymptotic fixed point analysis [3,8] provides an analytical understanding of the phenomenon observed in the numerical calculations.

On a finite momentum grid the scattering process becomes a bound-state problem [10] and many important properties such as the intertwining properties of the Moller wave operators do not hold. Actually, we will show that on the momentum grid the reaction matrix generally used to solve the Lippmann–Schwinger (LS) equation does not produce isospectral phase-shifts, i.e. $\delta^{LS}(H_0) \neq \delta^{LS}(U_\lambda H_0 U_\lambda^\dagger)$. There has been a renewed and continuous effort by Kukulin et al. [11,12] to formulate a new approach toward a direct evaluation of the multichannel multienergy S-matrix without solving the scattering equations in the few-body problem. These attempts can be traced from early work by Lifshits in the 1940s (see e.g. [11,12]) where quite generally the relevance of the energy-shift was established for impurities in a crystal. This is similar to the relation between the energy-shift and the phase-shift at large volumes [13,14]. Because of more recent popularity within lattice QCD calculations it is called the Luscher formula when the momentum grid is fixed by the finite lattice volume [15,16]. The energy-shift approach does comply to the isospectrality requirement, as it just involves the eigenvalues. In the continuum limit all these approaches are expected to fulfill Levinson's theorem (see e.g. [17] and references therein).

In the present paper we want to display an interesting connection between the SRG method in the infrared limit [8], which drives the system to a diagonal interaction, and the eigenvalue method for scattering which can be formulated without any reference to the SRG flow and the scattering equations. For a finite dimensional space with dimension N, there are $N!$ possible orderings for the eigenvalues of the diagonalized Hamiltonian and, as we will show, when bound-states occur picking the right ordering proves crucial to establish an energy-shift which allows to deduce phase-shifts embodying Levinson's theorem [17] in the continuum limit.

2. SRG on a momentum grid

The general SRG flow equation corresponds to a one-parameter operator evolution dynamics given by [18],

$$\frac{dH_s}{ds} = \left[[G_s, H_s], H_s \right], \tag{1}$$

and supplemented with a boundary condition, $\lim_{s \to 0} H_s = H_0$. As it is customary we will often switch from the flow parameter s to the SRG cutoff variable $\lambda = s^{-1/4}$ which has dimensions of momentum. The isospectrality of the SRG becomes evident from the trace invariance property $\mathrm{Tr}(H_s)^n = \mathrm{Tr}(H_0)^n$. The SRG generator G_s

can be chosen according to certain requirements, and here we will use two popular choices: the relative kinetic energy $G_s = T$, which is by construction independent of s [19] (Wilson generator), and the evolving diagonal part of the Hamiltonian $G_s = diag(H_s)$ [20] (Wegner generator). Normalizations are taken as in Ref. [21].

While the problem we address is fairly general, for illustration purposes we consider the toy model separable Gaussian potential discussed previously [22,23] which provides a reasonable description of the NN system in the $^1S_0$ and $^3S_1$ partial-wave channels at low-momenta, and support none or one (deuteron) bound state respectively. The action of the (bare) Hamiltonian on a given state in momentum space is given by (here and in what follows we use units such that $\hbar = c = M = 1$, where M is the nucleon mass)

$$H_0 \psi(p) = p^2 \psi(p) + \frac{2}{\pi} \int_0^\infty q^2 dq V_0(p,q) \psi(q). \tag{2}$$

The SRG flow equations are solved numerically on an N-dimensional momentum grid, $p_1 < \cdots < p_N$, by implementing a high-momentum ultraviolet (UV) cutoff, $p_{max} = \Lambda$, and an infrared (IR) momentum cutoff $p_{min} = \Delta p$ [21]. The integration rule becomes[1]

$$\int_{\Delta p}^{\Lambda} dp f(p) \to \sum_{n=1}^{N} w_n f(p_n). \tag{3}$$

The SRG flow equations on the grid follow from inserting the completeness relation in discretized momentum space

$$1 = \frac{2}{\pi} \sum_{n=1}^{N} w_n p_n^2 |p_n\rangle \langle p_n|. \tag{4}$$

For instance, the eigenvalue problem on the grid may be formulated as

$$H_\lambda \varphi_\alpha(p) = P_\alpha^2 \varphi_\alpha(p), \tag{5}$$

where the matrix representation of the Hamiltonian reads

$$H_\lambda(p_n, p_m) = p_n^2 \delta_{n,m} + \frac{2}{\pi} w_n p_n^2 V_\lambda(p_n, p_m). \tag{6}$$

A bound-state with (negative) eigenvalue $P_\alpha^2 = -B_\alpha$ corresponds to a pole in the scattering amplitude at imaginary momentum $P_\alpha = i\gamma$.

Because of the commutator structure of the SRG flow equation the isospectrality property still holds on the grid, i.e. $H_\lambda = U_\lambda H_0 U_\lambda^\dagger$, and therefore the eigenvalues P_α^2 of H_λ are λ-independent,

$$\frac{dP_\alpha}{d\lambda} = 0. \tag{7}$$

Although the eigenvalues are preserved along the SRG trajectory, the ordering of the states depends on the generator G of the SRG transformation. A lot of accumulated numerical experience has shown that in the presence of bound-states (real or spurious) Hamiltonians evolved using Wilson and Wegner generators start behaving differently when the SRG cutoff λ approaches some critical momentum Λ_c, which corresponds to the threshold scale where the bound-state emerges [24,25]. In the Wilson generator case the bound-state remains coupled to the low-momentum

---

[1] We take a Gauss–Legendre grid. The choice of grid is largely irrelevant for $N > 20$. Likewise, we could phrase the discretization problem in a harmonic oscillator basis, but the link to Levinson's theorem is less direct.

scales as λ approaches Λ_c, such that the bound-state eigenvalue is pushed towards the lowest momentum available on the grid, which corresponds to the IR momentum cutoff Δp. Moreover, when $\Delta p \to 0$ matrix-elements of the potential at low-momentum diverge in order to force the bound-state eigenvalue to smaller momenta, such that the SRG evolution may become numerically unstable. In the Wegner generator case the bound-state decouples from the low-momentum scales as λ approaches Λ_c, being placed on the diagonal of the Hamiltonian as an isolated negative eigenvalue at a momentum between the lowest momentum on the grid and Λ_c. As pointed out in Ref. [25], the *a priori* determination of the position at which the bound-state is placed on the diagonal when using Wegner generator is still an open problem. It is important to note that when the SRG cutoff λ is kept well above Λ_c or in the absence of bound-states the SRG evolution using Wilson and Wegner generators are nearly identical, a behavior that can be traced to the dominance of the kinetic energy.

One should note that the critical momentum scale Λ_c is distinct from the characteristic bound-state momentum scale γ. For weakly coupled bound-states, such as the deuteron, we can make an estimation of Λ_c by exploiting the complementarity between the implicit and explicit renormalization of effective interactions analyzed in Ref. [22]. This is based on using low-energy scattering data to encode the high-energy part of the interaction by imposing suitable renormalization conditions for an effective theory with a momentum cutoff scale Λ that divides the Hilbert space into a low-momentum P-space ($p < \Lambda$) and a high-momentum Q-space ($p > \Lambda$), separating explicitly what degrees of freedom and interactions behave dynamically. At low values of Λ the interaction can be expanded in powers of momenta ($p, p' < \Lambda$),

$$V(p', p) = C_0(\Lambda) + C_2(\Lambda)(p^2 + p'^2) + \cdots. \tag{8}$$

We can determine the low-energy constants $C_0, C_2, \ldots$ from low-energy data. For instance at leading-order (LO) we just fix the scattering length α_0 at *any* value of Λ which leads to the running of the coupling constant C_0 given by

$$C_0(\Lambda) = \frac{\alpha_0}{1 - \frac{2\Lambda\alpha_0}{\pi}}. \tag{9}$$

In this simple contact theory the deuteron wave function is given by the equation

$$\Psi_d(p) = \frac{Z}{p^2 + \gamma^2}, \tag{10}$$

where Z is determined from the normalization condition of the bound-state and fulfills the relation

$$Z\left(1 + \frac{2}{\pi}C_0(\Lambda)\int_0^\Lambda \frac{q^2}{q^2 + \gamma^2}dq\right) = 0. \tag{11}$$

Clearly, in order to get a non-trivial solution $Z \neq 0$ the coupling constant C_0 must be negative. As we see this requires $\alpha_0 > 0$ and $\Lambda > \Lambda_c^{LO} = 2/\pi\alpha_0$. Taking $\alpha_0 = 5.42$ fm for the $^3S_1$ channel we obtain $\Lambda_c^{LO} \sim 0.3$ fm^{-1}. The calculation at next-to-leading-order (NLO) further determines $C_2(\Lambda)$ from the effective range $r_0 = 1.75$ fm [22] and the deuteron wave function in Eq. (10) is modified by replacing $Z \to Z(1 + Xq^2)$ and after solving for X provides a tiny correction, $\Lambda_c^{NLO} = 0.29$ fm^{-1}. A different variational estimate can be done by looking at what Λ the matrix Hamiltonian in the P-space supports a bound state.

The emergence of the threshold scale Λ_c is displayed in Fig. 1, where the characteristic deuteron momentum scale γ is shown as a function of the cutoff Λ for the variational and the implicit renormalization estimates. In Fig. 1 we also see that the
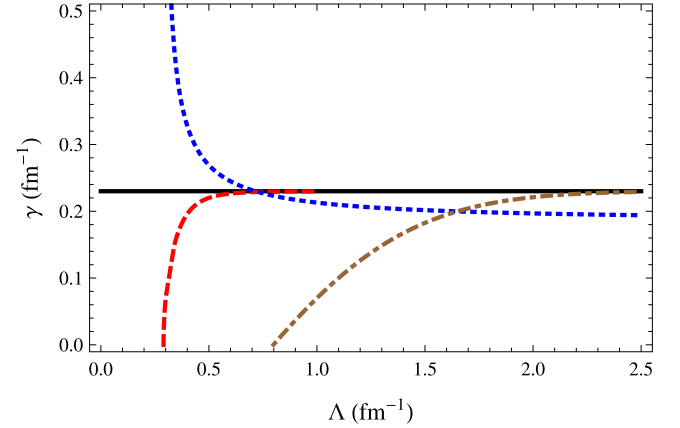

Fig. 1. Variational (dotted–dashed) and implicit (LO: dotted, NLO: dashed) determinations of the critical momentum scale Λ_c above which the interaction supports a bound state, $P^2 = -B = -\gamma(\Lambda)^2$. The full Hamiltonian has $\lim_{\Lambda\to\infty}\gamma(\Lambda) = \gamma_d = 0.23$ fm^{-1} corresponding to the deuteron (solid). The critical value Λ_c corresponds to $\gamma = 0$. Note that in the LO case, since the interaction is purely attractive, the threshold cutoff gives $\gamma = \infty$.

NLO approximation saturates at the exact value of γ for $\Lambda \sim 2\Lambda_c$. The performance of the variational approach, for the model under study, is not good. Actually, large values of Λ are needed to saturate the bound state. Note that the exact solution would have a discontinuity at the exact Λ_c.

In Fig. 2 we show the SRG evolution of the lowest diagonal matrix elements of the toy model Hamiltonian $H_{n,n}^{G,\lambda}$ ($n = 1, \ldots, 6$) in the $^1S_0$ and $^3S_1$ partial-wave channels, for a momentum grid with $N = 20$ points and $\Lambda = 2$ fm^{-1}. The SRG cutoff λ was varied in a range from 0.05 to 2.0 fm^{-1}. An interesting difference can be observed between the SRG evolution with Wilson and Wegner generators in the infrared limit. As the SRG cutoff λ approaches the critical momentum scale Λ_c, there is no crossing amongst the diagonal matrix elements for the $^1S_0$ channel both with Wilson and Wegner generators indicating that the initial ascending order is maintained all along the SRG trajectory. Moreover, both generators lead to similar SRG evolutions, as expected since there are no bound-states. For the $^3S_1$ channel, on the other hand, there are crossings with both generators. In the Wilson generator case the initial ascending order is asymptotically restored in the limit $\lambda \to 0$ [3,8] with the lowest momentum diagonal matrix element $H_\lambda(p_1, p_1)$ flowing into the deuteron bound-state. In the Wegner generator case a re-ordering occurs with some upper momentum diagonal matrix element $H_\lambda(p_{n_{BS}}, p_{n_{BS}})$ flowing into the deuteron bound-state in the limit $\lambda \to 0$. As shown in Ref. [25] for LO chiral effective field theory (EFT) interactions with large momentum cutoffs Λ_{EFT}, the position at which the (spurious) bound-state is placed changes with the cutoff. In our calculations for the separable Gaussian toy model potential on a finite momentum grid we observe a similar change of the bound-state position when using different values for the number of grid points N and/or the high-momentum UV cutoff Λ. For the calculation with $N = 20$ grid points and $\Lambda = 2$ fm^{-1}, shown in Fig. 2, the momentum at which the bound-state is placed corresponds to $p_{n_{BS}} \to p_5 \sim 0.254$ fm^{-1}. As one can observe, the diagonal matrix-element $H_\lambda(p_{BS}, p_{BS})$ that flows into the deuteron bound-state is the one that starts to decrease rapidly towards negative values when the SRG cutoff λ approaches $\Lambda_c \sim 0.3$ fm^{-1}, indicating the break-up of the kinetic energy dominance, i.e.

$$p_{n_{BS}}^2 < \frac{2}{\pi}w(p_{n_{BS}})p_{n_{BS}}^2\big|V_{\lambda<\Lambda_c}(p_{n_{BS}}, p_{n_{BS}})\big|. \tag{12}$$
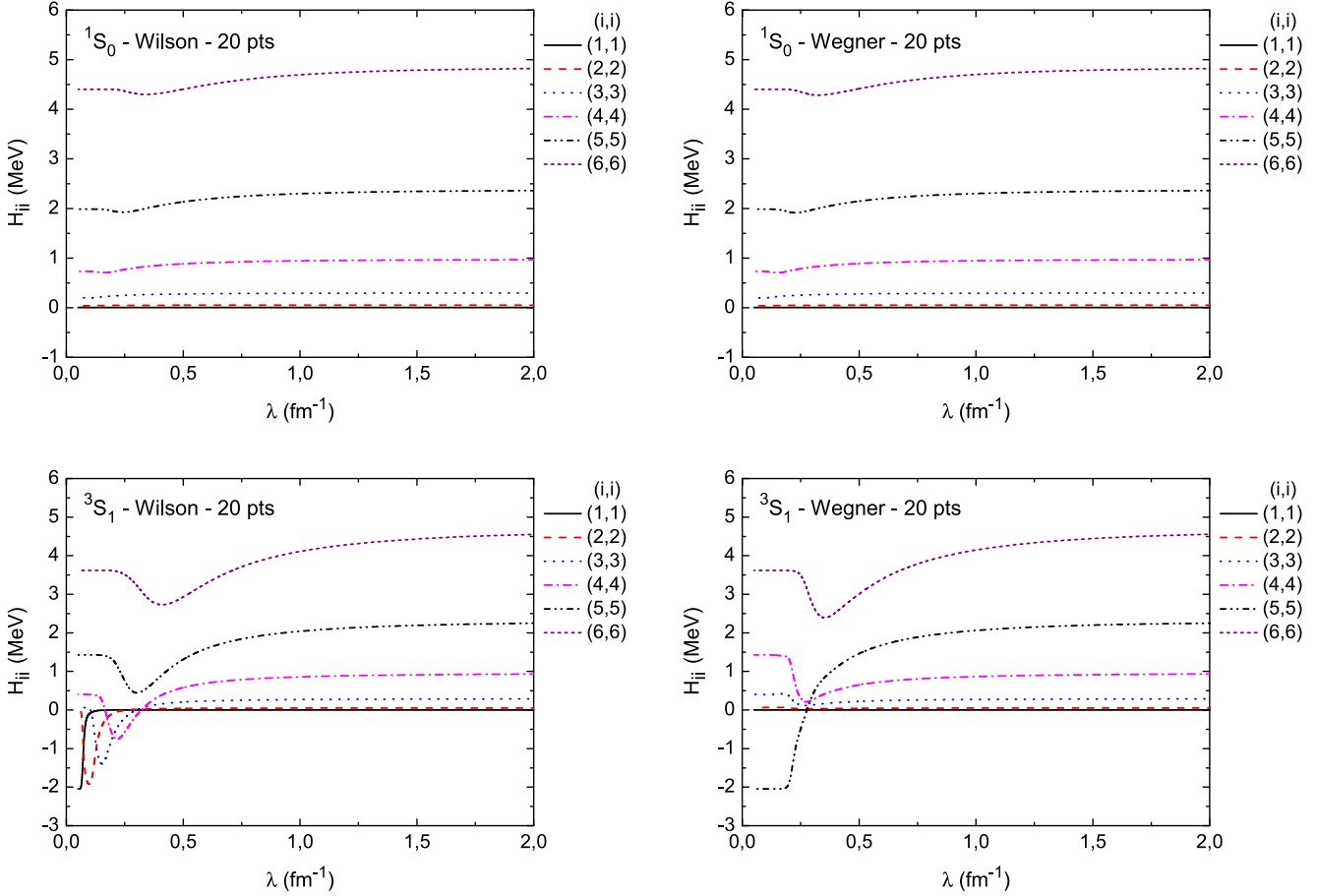
Fig. 2. SRG evolution of the diagonal matrix-elements of the Hamiltonian for the toy model potential in the $^1S_0$ (upper panels) and $^3S_1$ (lower panels) channels using the Wilson (left) and the Wegner (right) generators. We have considered a high-momentum UV cutoff $\Lambda = 2$ fm^{-1} and $N = 20$ grid points. The SRG cutoff λ was varied in a range from 0.05 to 2.0 fm^{-1}.

3. Phase-inequivalence of the reaction matrix on a momentum grid

As mentioned above the original motivation for the SRG method was to soften the interaction while keeping the phase-shifts invariant. As we will show below the verification of phase-equivalence along the SRG trajectory requires a proper definition of the phase-shift in a momentum grid. This is a subtle point, particularly when the interaction is attractive enough to generate bound states.

The standard procedure so far within the SRG approach has been to solve the Lippmann–Schwinger (LS) equation for the T-matrix. In operator form the LS equation reads

$$T = V + V\left(p^2 - H_0 - i\epsilon\right)^{-1}T. \tag{13}$$

Taking matrix elements on the momentum grid we get

$$T_{nm}(p) = V_{nm} + \frac{2}{\pi}\sum_{k=1}^{N} w_k \frac{p_k^2}{p^2 - p_k^2 + i\epsilon} V_{nk}T_{k,m}(p), \tag{14}$$

where p^2 is the scattering energy. The on-shell limit is obtained by taking $p = p_l$ on the grid. As usual we switch to the reaction matrix which on the grid yields the equation for the half-on-shell amplitude

$$R_{nm}(p_m) = V_{nm} + \frac{2}{\pi}\sum_{k\neq m} w_k \frac{p_k^2}{p_m^2 - p_k^2} V_{nk}R_{k,m}(p_m), \tag{15}$$

where the excluded sum embodies the principal value prescription of the continuum version. This equation can be solved by inversion for any grid point p_n and thus we may obtain the phase-shifts

$$-\frac{\tan\delta^{LS}(p_n)}{p_n} = R_{nn}(p_n), \tag{16}$$

where the supper-script LS denotes that these phase-shifts are obtained from the solution of the LS equation on the grid. Of course, the limit $N \to \infty$ should be understood in the end.

Let us analyze the behavior of the phase-shifts as computed from the definition given in Eq. (16) using the potentials $V_{nm}(\lambda)$ evolved according to the SRG flow equations, Eq. (1), on the finite grid. The results for the toy model potential in the $^1S_0$ (left) and $^3S_1$ (right) channels are presented in Fig. 3 for a high-momentum UV cutoff $\Lambda = 2$ fm^{-1}, $N = 30$ grid points and several values of the SRG cutoff λ. As we see, Levinson's theorem [17], $\delta_\lambda^{LS}(p_1) - \delta_\lambda^{LS}(p_N) = n_B\pi$, is fulfilled on the grid. However, while this discretization enables to handle SRG flow equations numerically, the price to pay due to the finite momentum grid, however, is that on this grid the phase-shifts as obtained from the LS equation are not independent of the SRG cutoff variable λ. While the lack of phase-equivalence disappears for large N we want to analyze the possibility whether one can define SRG-independent phase-shifts on the grid for *any* value of the dimension N.
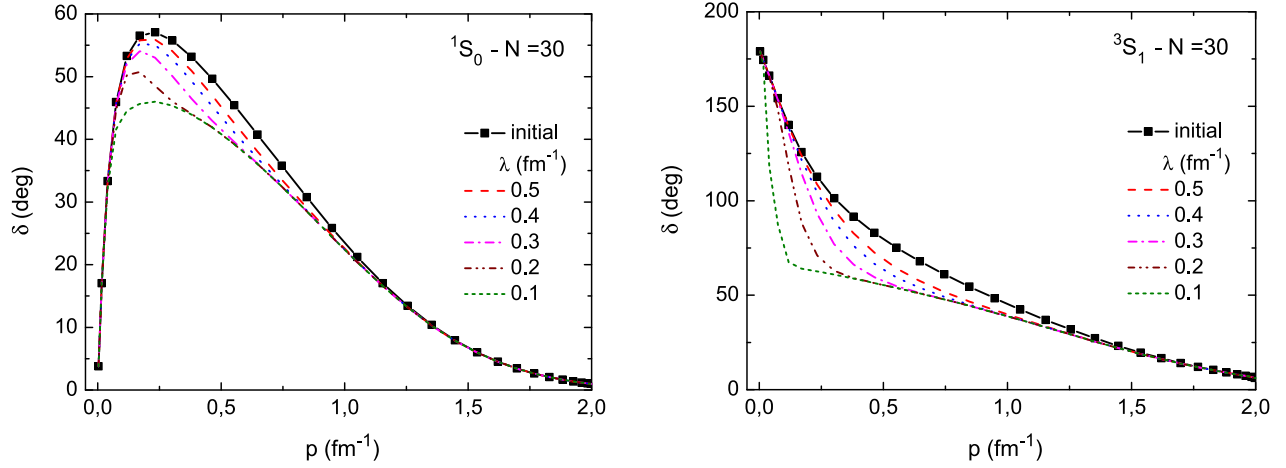
Fig. 3. Phase-shifts evaluated from the solution of the LS equation on the momentum grid with the toy model potential in the $^1S_0$ (left) and $^3S_1$ (right) channels evolved through the SRG transformation with Wilson generator for several values of the SRG cutoff λ. We have considered a high-momentum UV cutoff $\Lambda = 2$ fm^{-1} and $N = 30$ grid points.

4. The energy-shift operator

The most obvious phase-shift definition preserving phase-equivalence on the grid should involve the spectrum. Fortunately, this was done long ago by Lifshits and has recently received a lot of attention by Kukulin et al. who extended the energy-shift approach to few-nucleon problems [11,12]. Their setup allows to solve scattering problems without ever solving the scattering equations, since it just involves the energy eigenvalues. It is important to note that for an N-dimensional momentum grid there are $N!$ possible orderings for the eigenvalues of the Hamiltonian obtained from any diagonalization procedure and so the evaluation of phase-shifts using the energy-shift approach necessarily involves a prescription to order the states.

The general result in the presence of n_B bound-states derived by Kukulin et al. is written as

$$\delta_n^{\text{Kuk}} = -\pi \frac{P_{n+n_B}^2 - p_n^2}{2w_n p_n}, \tag{17}$$

with $n = 1, \ldots, N - n_B$. According to this prescription, in order to evaluate the phase-shifts the eigenvalues P_n^2 obtained from the diagonalization of the Hamiltonian H (arranged in ascending order) must be shifted to the left by n_B positions with respect to the corresponding eigenvalues p_n^2 of the free Hamiltonian T. One should note that such a prescription implies that the first n_B eigenvalues (those corresponding to the bound-states) are removed when the shift is implemented. The results obtained by applying Eq. (17) to evaluate the phase-shifts for the toy-model potential in the $^1S_0$ and $^3S_1$ channels with several number of grid points N can be seen in Fig. 4. In the case of the $^1S_0$ channel, which has no bound-state, there is no shift of the eigenvalues P_n^2 since $n_B = 0$ and the prescription works rather well in the entire range of momenta as one can see in the upper-left panel. The situation for the $^3S_1$ channel is different since $n_B = 1$ due to the presence of the deuteron bound-state. As we can see in the left-bottom panel, when no shift is applied the low-momenta behavior clearly violates Levinson's theorem. As shown in the upper-right panel, the low-momenta behavior is properly fixed by shifting the eigenvalues according to Kukulin's prescription and looks like fulfilling Levinson's theorem for one bound-state. However, the large momentum behavior is greatly distorted due to the mismatch of the free momenta and the eigenvalues generated by the shift. This effect survives in the continuum limit and the upper bending indicates that Levinson's

theorem is fulfilled, however, with no bound states. Thus we are faced to the problem of defining an isospectral phase-shift with a proper high-energy behavior.

Clearly, in order to avoid the high-energy mismatch the constant shift implied by Kukulin's formula should not be used. On the other hand, the shifted formula complies to Levinson's theorem at low-energies. Thus, even within the isospectral scenario there seems to be a conflict between high-energy behavior and the fulfillment of Levinson's theorem. Therefore, the question is at what location should the shift of the eigenvalues be applied in order to obtain phase-shifts that have a proper behavior both at low-energies and high-energies.

5. The SRG induced ordering of states

As pointed out before, in the case of the SRG evolution with Wilson generator there is only one asymptotically stable final ordering of the eigenvalues, corresponding to the permutation in which the eigenvalues are ordered according to the kinetic energy (i.e., in ascending order). On the other hand, the SRG evolution with Wegner generator allows in principle any asymptotically stable final ordering of the eigenvalues. However, the uniqueness of the solution implies that just one ordering takes place asymptotically for $\lambda \to 0$. In the absence of bound-states, the final ordering for the Wegner generator is the same as for the Wilson generator (ascending order).

We define the SRG-ordered phase-shift for the generator G as follows

$$\delta_n^G = -\pi \lim_{\lambda \to 0} \frac{H_{n,n}^{G,\lambda} - p_n^2}{2w_n p_n}. \tag{18}$$

If we denote by E_n the spectrum of $H_{n,n}^{G,\lambda}$ in ascending order, i.e. $E_1 < \cdots < E_N$, we generally have

$$\lim_{\lambda \to 0} H_{n,m}^{G,\lambda} = \delta_{n,m} E_{\pi(n)} = \delta_{n,m} P_{\pi(n)}^2, \tag{19}$$

where $\pi(n)$ is one of the $N!$ permutations of the N-plet $(1, \ldots, N)$.

For the Wilson generator, $G_s = T$, one can show that the ascending order is asymptotically preserved [3,8],

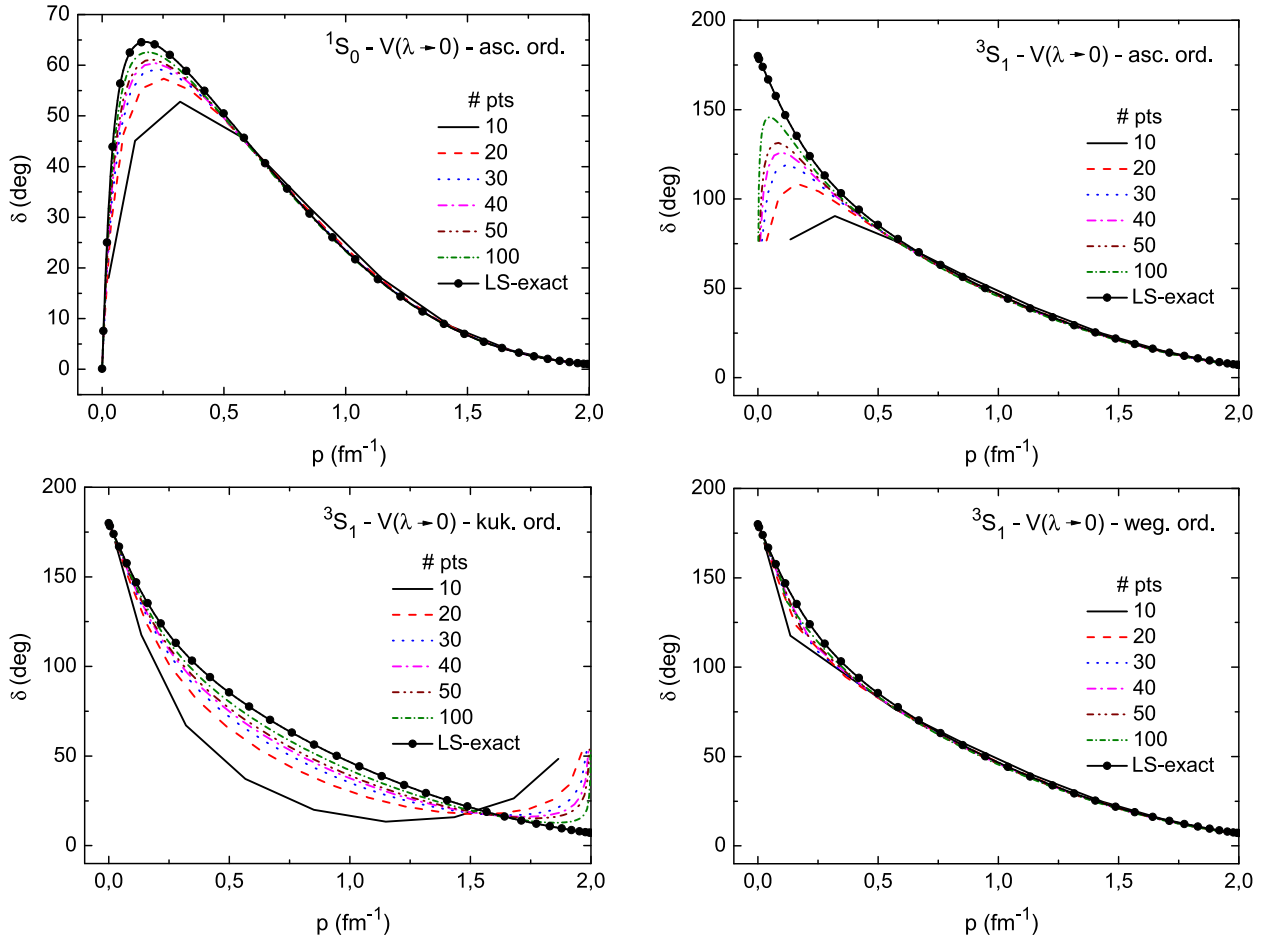$$\lim_{\lambda \to 0} H_{n,m}^{\text{Wil},\lambda} = \delta_{n,m} E_n, \tag{20}$$

Fig. 4. Phase-shifts for the toy model potential in the $^1S_0$ and $^3S_1$ channels evaluated by the eigenvalue method with the eigenvalues sorted in several ways. Upper left panel: $^1S_0$ channel in ascending order. Upper right panel: $^3S_1$ channel in ascending order. Lower left panel: $^3S_1$ channel with Kukulin et al. order. Lower right panel: $^3S_1$ channel in permuted ordering. Some of these orderings can be identified with Wilson or Wegner SRG generators when the infrared limit is taken $\lambda \to 0$. We have considered a high-momentum UV cutoff $\Lambda = 2$ fm^{-1} and different number of grid points $N = 10, 20, 30, 40, 50, 100$. The points corresponding to the momentum at which the deuteron bound-state eigenvalue is placed on the diagonal of the Hamiltonian are omitted. We also show the exact phase-shifts obtained from the solution of the standard LS equation.

and thus

$$\delta_n^{\mathrm{Wil}} = -\pi \lim_{\lambda \to 0} \frac{H_{n,n}^{\mathrm{Wil},\lambda} - p_n^2}{2 w_n p_n} = -\pi \frac{P_n^2 - p_n^2}{2 w_n p_n} \qquad (21)$$

which corresponds to Kukulin's formula with no shift and thus leads to the violation of Levinson's theorem in the presence of bound-states.

For the Wegner generator case, $G_s = diag(H_s)$,

$$\delta_n^{\mathrm{Weg}} = -\pi \lim_{\lambda \to 0} \frac{H_{n,n}^{\mathrm{Weg},\lambda} - p_n^2}{2 w_n p_n}. \qquad (22)$$

Our analysis of the results obtained for the SRG evolution of the toy-model Hamiltonian, shown in Fig. 2, suggests an alternative prescription to order the eigenvalues when using the energy-shift approach to evaluate the phase-shifts. By placing the bound-state eigenvalue at the position induced by the SRG evolution with Wegner generator in the infrared limit ($\lambda \to 0$), which corresponds to the grid momentum $p_{n_{\mathrm{BS}}}$, we have

$$\lim_{\lambda \to 0} H_{n,m}^{\mathrm{Weg},\lambda} = \delta_{n,m} \begin{cases} P_{n+1}^2 & \text{if } n < n_{\mathrm{BS}}, \\ -\gamma^2 & \text{if } n = n_{\mathrm{BS}}, \\ P_n^2 & \text{if } n < n_{\mathrm{BS}}. \end{cases} \qquad (23)$$

Literal application of this result in Eq. (22) generates a discontinuity at $\delta_{n_{\mathrm{BS}}}$. We can instead just remove the point at the position

$n = n_{\mathrm{BS}}$ corresponding to the location of the bound-state eigenvalue, similar to what is done in Kukulin's prescription, or interpolate between the neighboring values, taking $P_{n_{\mathrm{BS}}}^2 \to \bar{P}_{n_{\mathrm{BS}}}^2 = (P_{n_{\mathrm{BS}}+1}^2 + P_{n_{\mathrm{BS}}-1}^2)/2$. This yields

$$\bar\delta_n^{\mathrm{Weg}} = \begin{cases} -\pi \frac{P_{n+1}^2 - p_n^2}{2 w_n p_n} & \text{if } n < n_{\mathrm{BS}}, \\ -\pi \frac{\bar{P}_n^2 - p_n^2}{2 w_n p_n} & \text{if } n = n_{\mathrm{BS}}, \\ -\pi \frac{P_n^2 - p_n^2}{2 w_n p_n} & \text{if } n > n_{\mathrm{BS}}. \end{cases} \qquad (24)$$

In this way, we get an ordering prescription in which *only* the eigenvalues corresponding to momenta $p_n < p_{n_{\mathrm{BS}}}$ are shifted one position to the left, unlike Kukulin's prescription in which *all* eigenvalues are shifted. As pointed before, the position of the bound-state eigenvalue induced by the SRG evolution with Wegner generator changes when using different values for the number of grid points N and so the momentum $p_{n_{\mathrm{BS}}}$ below which the shift is applied. In the bottom-right panel of Fig. 4 we show the phase-shifts evaluated from Eq. (24) for different number of grid points N, compared to the exact results obtained from the solution of the standard LS equation. As one can see, both low-energy and high-energy behaviors are correct within the expected uncertainties of the finite grid. The good job performed by the SRG evolution with Wegner generator in properly locating the momentum $p_{n_{\mathrm{BS}}}$
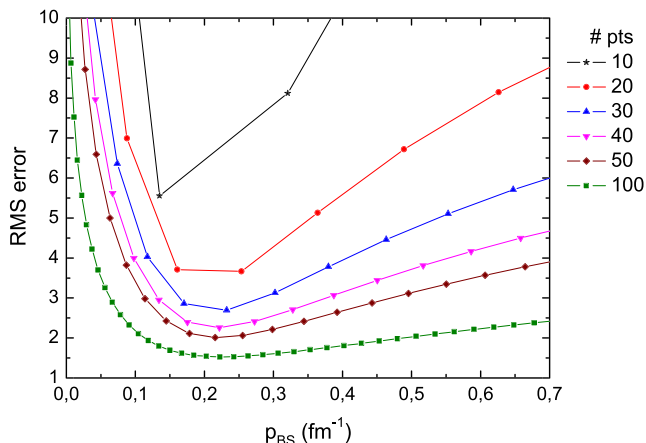
Fig. 5. RMS errors in the phase-shifts (in degrees) for the toy model potential in the $^3S_1$ channel evaluated from the energy-shift formula by varying the position of the deuteron bound-state eigenvalue. We have considered a high-momentum UV cutoff $\Lambda = 2$ fm^{-1} and different number of grid points $N = 10, 20, 30, 40, 50, 100$.

Table 1
Comparison between the position of the deuteron bound-state which minimizes the RMS errors in the phase-shifts, $p_{n_{BS}}^{\text{opt}}$, and the position induced by the SRG evolution with Wegner generator in the infrared limit, $p_{n_{BS}}^{\text{weg}}$, for different number of grid points $N = 10, 20, 30, 40, 50, 100$.

N	$p_{n_{BS}}^{\text{opt}}$ (fm^{-1})	$p_{n_{BS}}^{\text{weg}}$ (fm^{-1})
10	0.135	0.321
20	0.254	0.254
30	0.232	0.170
40	0.221	0.175
50	0.215	0.145
100	0.222	0.104

at which the bound-state eigenvalue must be placed when using the energy-shift approach can be traced to the decoupling of the bound-state from the low-momentum scales in the infrared limit.

Thus, we find that remarkably the ordering of the eigenvalues induced by the SRG evolution with Wegner generator in the infrared limit provides a prescription which allows to obtain isospectral phase-shifts that fulfill Levinson's theorem at low-momenta and have a proper behavior at high-momenta. However, such an ordering does not correspond in general to the optimal one. We have evaluated the phase-shifts for the toy model potential in the $^3S_1$ channel from the energy-shift formula by varying the position of the deuteron bound-state eigenvalue $p_{n_{BS}}$ and compared to the exact results obtained from the solution of the standard LS equation. In Fig. 5 we show the plots corresponding to the RMS errors *versus* $p_{n_{BS}}$ computed for several number of grid points N. As one can see in Table 1, the position of the deuteron bound-state which minimizes the RMS errors, $p_{n_{BS}}^{\text{opt}}$, is different from the position induced by the SRG evolution with Wegner generator in the infrared limit, $p_{n_{BS}}^{\text{weg}}$. Since the SRG evolution with distinct generators induces different isospectral flows in the presence of bound-states, it is plausible to conceive that a specific generator may be found which leads to the optimal ordering. It is also interesting to note that in the continuum limit the position of the deuteron bound-state which minimizes the RMS errors seems to approach the characteristic deuteron momentum scale $\gamma = 0.23$ fm^{-1}. Of course, it must be verified through explicit calculations if this is a general result, which holds for any weakly or strongly coupled bound-state.

6. Conclusions

We have unveiled a remarkable connection between the SRG evolution for a generic generator and the Levinson theorem on a finite momentum grid, where the scattering problem turns into a bound state problem. So some naive relations such as the phase-equivalence of the transformation depend on the very definition of the phase-shift and certainly do not hold for the customary Lippmann–Schwinger definition. An isospectral definition is based on an energy shift due to the interaction and is phase-equivalent along the SRG trajectory, but different generators provide different eigenvalue orderings and fulfilling Levinson's theorem depends on knowledge of the location of a bound state scale in momentum space. We have seen that while the Wilson generator induces an ordering contradicting Levinson's theorem, the Wegner generator does a much better job, but still underestimates the relevant momentum scale. The main handicap to the general analysis seems to be that within the matrix formulation it is difficult to profit of the specific information embodied in quantum mechanical Hamiltonians. A more rigorous discussion will probably implement asymptotic and analytic features of the Hamiltonian as a function of the momentum and in the complex plane. We remind that the standard proof of Levinson's theorem in the continuum makes extensive use of these features [17].

For the case under study we restrict ourselves to the one single bound state situation, which actually corresponds to the case of interest in the two nucleon problem. We have also checked that our prescription works also for realistic potentials. Our results should find a sensible generalization for more bound states, and we leave this study for future investigation.

Acknowledgements

References

[1] S. Bogner, R. Furnstahl, R. Perry, Similarity renormalization group for nucleon–nucleon interactions, Phys. Rev. C 75 (2007) 061001.
[2] R. Furnstahl, K. Hebeler, New applications of renormalization group methods in nuclear physics, Rep. Prog. Phys. 76 (2013) 126301, http://dx.doi.org/10.1088/0034-4885/76/12/126301, arXiv:1305.3800.
[3] V. Timoteo, S. Szpigel, E. Ruiz Arriola, Symmetries of the similarity renormalization group for nuclear forces, Phys. Rev. C 86 (2012) 034002, http://dx.doi.org/10.1103/PhysRevC.86.034002, arXiv:1108.1162.
[4] E. Ruiz Arriola, V. Timoteo, S. Szpigel, Nuclear symmetries of the similarity renormalization group for nuclear forces, PoS CD12 (2013) 106, arXiv:1302.3978.
[5] B. Dainton, R. Furnstahl, R. Perry, Universality in similarity renormalization group evolved potential matrix elements and T-matrix equivalence, Phys. Rev. C 89 (2014) 014001, http://dx.doi.org/10.1103/PhysRevC.89.014001, arXiv:1310.6690.
[6] R.N. Perez, J. Amaro, E.R. Arriola, Coarse grained potential analysis of neutron–proton and proton–proton scattering below pion production threshold, Phys. Rev. C 88 (2013) 064002, http://dx.doi.org/10.1103/PhysRevC.88.064002, arXiv:1310.2536.
[7] A. Bulgac, M.M. Forbes, On the use of the discrete variable representation basis in nuclear physics, Phys. Rev. C 87 (2013) 051301, http://dx.doi.org/10.1103/PhysRevC.87.051301, arXiv:1301.7354.
[8] E. Ruiz Arriola, S. Szpigel, V. Timoteo, Fixed points of the similarity renormalization group and the nuclear many-body problem, Few-Body Syst. (2014), http://dx.doi.org/10.1007/s00601-014-0858-7, arXiv:1310.8246.
[9] K. Hebeler, Momentum space evolution of chiral three-nucleon forces, Phys. Rev. C 85 (2012) 021002, http://dx.doi.org/10.1103/PhysRevC.85.021002.
[10] J. Muga, R. Levine, Stationary scattering theories, Phys. Scr. 40 (2) (1989) 129.

[11] V.I. Kukulin, V.N. Pomerantsev, O.A. Rubtsova, Discrete representation of the spectral shift function and the multichannel *s*-matrix, JETP Lett. 90 (5) (2009) 402–406.

[12] O. Rubtsova, V. Kukulin, V. Pomerantsev, A. Faessler, New approach toward a direct evaluation of the multichannel multienergy S matrix without solving the scattering equations, Phys. Rev. C 81 (2010) 064003, http://dx.doi.org/10.1103/PhysRevC.81.064003.

[13] N. Fukuda, R. Newton, Energy level shifts in a large enclosure, Phys. Rev. 103 (1956) 1558–1564, http://dx.doi.org/10.1103/PhysRev.103.1558.

[14] B.S. DeWitt, Transition from discrete to continuous spectra, Phys. Rev. 103 (1956) 1565–1571, http://dx.doi.org/10.1103/PhysRev.103.1565.

[15] M. Luscher, Volume dependence of the energy spectrum in massive quantum field theories. 1. Stable particle states, Commun. Math. Phys. 104 (1986) 177, http://dx.doi.org/10.1007/BF01211589.

[16] M. Luscher, Two particle states on a torus and their relation to the scattering matrix, Nucl. Phys. B 354 (1991) 531–578, http://dx.doi.org/10.1016/0550-3213(91)90366-6.

[17] Z.-Q. Ma, The Levinson theorem, J. Phys. A 39 (2006) R625–R659, http://dx.doi.org/10.1088/0305-4470/39/48/R01.

[18] S. Kehrein, The Flow Equation Approach to Many-Particle Systems, Springer, 2006.

[19] F. Wegner, Flow-equations for Hamiltonians, Ann. Phys. 506 (2) (1994) 77–91.

[20] S.D. Glazek, K.G. Wilson, Perturbative renormalization group for Hamiltonians, Phys. Rev. D 49 (1994) 4214–4218.

[21] S. Szpigel, V.S. Timoteo, F.d.O. Duraes, Similarity renormalization group evolution of chiral effective nucleon–nucleon potentials in the subtracted kernel method approach, Ann. Phys. 326 (2011) 364–405, http://dx.doi.org/10.1016/j.aop.2010.11.007, arXiv:1003.4663.

[22] E. Ruiz Arriola, S. Szpigel, V. Timoteo, Implicit vs explicit renormalization and effective interactions, Phys. Lett. B 728 (2014) 596–601, http://dx.doi.org/10.1016/j.physletb.2013.12.038, arXiv:1307.1231.

[23] E.R. Arriola, S. Szpigel, V.S. Timoteo, Implicit vs explicit renormalization of the *NN* force, Few-Body Syst. (2014), http://dx.doi.org/10.1007/s00601-014-0811-9, arXiv:1310.8526.

[24] S.D. Glazek, R.J. Perry, The impact of bound states on similarity renormalization group transformations, Phys. Rev. D 78 (2008) 045011, http://dx.doi.org/10.1103/PhysRevD.78.045011, arXiv:0803.2911.

[25] K. Wendt, R. Furnstahl, R. Perry, Decoupling of spurious deep bound states with the similarity renormalization group, Phys. Rev. C 83 (2011) 034005, http://dx.doi.org/10.1103/PhysRevC.83.034005, arXiv:1101.2690.